Adaptive Droop control for voltage and frequency regulation in isolated microgrids

Gerônimo Barbosa Alexandre [1], Gabriel da Silva Belém [2]

[1] geronimo.alexandre@garanhuns.ifpe.edu.br. Instituto Federal de Educação, Ciência e Tecnologia de Pernambuco (IFPE), *campus* Garanhuns, Departamento de Engenharia Elétrica. [2] gabrielsbgr@gmail.com. Instituto Federal de Educação, Ciência e Tecnologia de Pernambuco (IFPE), *campus* Garanhuns, Departamento de Engenharia Elétrica.

ABSTRACT

This paper proposes an adaptive droop control strategy for simultaneous regulation of voltage and frequency in isolated microgrids to meet the relevant legislation (NBR 5410 and IEEE 1547). The technique is based on the traditional structure of the Droop control (P-f) and (Q-V), aided by recursive least squares methods to estimate the line parameters. The control law is adaptive because the controller gains are self-adjusting to the operating conditions imposed by the loads and the legal restrictions for fluctuations in voltage and frequency in the microgrid. The controller was validated in different microgrids (1-bus, 3-bus, and IEEE 14-bus) and different types of loads. The simulation results show the effectiveness of the controller: rapid response in the accommodation of variations in loads; active power-sharing between the inverters and; stable and safe operation of the microgrid.

Keywords: Droop control. Optimum tuning. Parametric identification. Stable operation.

RESUMO

Este artigo propõe uma estratégia de controle Droop adaptativa para regulação simultânea de tensão e frequência em microgrids isoladas visando atender a legislação vigente (NBR 5410 e IEEE 1547). A técnica é baseada na estrutura tradicional do controle Droop (P-f) e (Q-V), auxiliada pelo método do mínimos quadrados recursivo para estimar os parâmetros da linha. A lei de controle é adaptativa pois os ganhos do controlador são auto ajustáveis as condições operacionais impostas pelas cargas e as restrições legais para as flutuações da tensão e da frequência na microgrid. O controlador foi validado em diferentes microgrids (1-bus, 3- bus e IEEE 14-bus) e diferentes tipos de cargas. Os resultados de simulação comprovam a eficácia do controlador: resposta rápida na acomodação das variações das cargas; compartilhamento de potência ativa entres os inversores; operação estável e segura da microgrid.

Palavras-chave: *Controle Droop. Sintonia ótima. Identificação paramétrica. Operação estável.*

 SUBMETIDO 22/07/2020 > APROVADO 28/09/2020

1 Introduction

The popularity of decentralized generation in Brazil can explain by the following factors: (a) advances in technologies associated with renewable sources and in the power electronics used; (b) the successive increase in the electricity bill charged by the local electricity concessionaires; (c) cheapening of related technologies and (d) funding from the government for low-income consumers.

In Brazil, the legal framework of distributed generation is the normative resolution n° 482 of 17 April of 2012, laying down general conditions for micro-generation access and mini distributed generation to power distribution systems and the electric energy compensation system.

A microgrid (MG), which includes locally distributed generators (DG) and loads, can operate in two different modes of operation. In interconnected mode it is connected to the main upstream grid, being supplied from or injecting power into it. Another mode is autonomous mode of operation and the microgrid is disconnected from distribution network (MAJUMDER; GHOSH; LEDWICH; ZARE, 2009; BALAGUER *et al.*, 2011).

Distributed generators improve service reliability and decrease the need for future generation expansion planning. Moreover, in concept of islanding microgrid, it extends up the possibility of making sources responsible for local power quality factors in a way that is not conceivable with conventional centralized power generation (MARWALI; KEYHANI, 2004; ZHENGBO; LINCHUAN; TUO, 2011; FU *et al.*, 2012).

In microgrids operating in isolated mode, dynamic load switching introduces fluctuations in voltage and frequency and loss of synchronism between the various installed microgenerators (GUERRERO *et al.*, 2011; BEVRANI; SHOKOOHI, 2013; HAGHSHENAS; EBADIN; SHARIATINASAB, 2014). Usually, the problem of synchronism is solved with the use of existing synchronous machines. However, as in MG isolated, there are these elements, the problem should solve by the local control system of each micro-generator. Moreover, these controllers are also responsible for the apparent power-sharing between the drives present in MG (MOHAMED; EL-SAADANY, 2008; ZHONG, 2011).

In this context, the commitment of the control solution consists of:

a) To maintain the balance between generation and consumption imposed by the IEEE 1547/2003 (standard for interconnecting distributed resources with electric power systems) for the interconnection requirements before the abrupt switching of loads (INSTITUTE OF ELECTRIC AND ELECTRONICS ENGINEERS, 2003);

b) Maintain the voltage and frequency within the operational range ($\Delta f = \pm 1$ Hz and $\Delta V = \pm 10$ V) prescribed by Brazilian standard NBR 5410/2004, low voltage electrical installations (ASSOCIAÇÃO BRASILEIRA DE NORMAS TÉCNICAS, 2004), during the MG operation in closed-loop;

c) Reducing the levels of harmonics injected by the DG's microgrid (THD < 5% and IHD < 3%) to meet IEEE 519/2014 (INSTITUTE OF ELECTRIC AND ELECTRONICS ENGINEERS, 2014).

In this paper, a new control structure proposed for simultaneous regulation of voltage and frequency in MG's in the face of dynamic load switching or when is lost connection to the medium-voltage network. The strategy uses the structure of the conventional droop associated with a recursive estimator (Recursive Least Squares – RLS) of parameters of the electrical network (plant).

The designed controller is a self-tuning regulator in the direct configuration. The parameters of the plant model adjusted online by the recursive estimator, least squares method, they sent to the tuning block controller, updating the gains of droop control law.

The plant model obtained by parameter estimator from the real-time voltage and current measurements provided by DG to the microgrid. In terms of electrical circuits, the Thevenin equivalent seen by the DG terminal, being approached by a second-order model.

The control strategy was evaluated in different load switching scenarios and different topologies of isolated microgrids (1-bus, 3-bus, and 14-bus).

The contributions of this paper are:

- Adaptive droop controller design for simultaneous regulation of voltage and frequency;
- Methodology for tuning the controller, based on MG operating conditions;
- Use of the recursive least-squares method to estimate the MG line parameters;
- Mathematical formulation of the control region and operational stability of MG;
- Determination of minimum conditions for sample update rates for each microgrid component.

To guide the reader, the paper divided into five sections that support a better understanding of the proposed solution for the regulation of voltage and frequency in smart grids.

Section 1 provides a general explanation of the voltage and frequency regulation problem in distribution networks with the penetration of distributed sources. In this scenario, there will be an increase in voltage and loss of synchronism on the part of the distributed generators, causing the distribution system to become unstable and not to comply with current legislation.

Section 2 dedicated to the mathematical formulation of the regulation solution based on simultaneous droop control of voltage and frequency in each distributed generator. The details of the smart droop control strategy presented in section 3. Section 4 presents the simulation results to validate the adaptive control in different test scenarios, focusing on grid stability and physical implementation of the embedded controller in the DC-AC converter. Finally, in section 5, we present the conclusions and possible future work.

1.1 Related works

The problem of voltage regulation in isolated MG's can be solved in several different ways (LOPES; MADUREIRA; MADUREIRA, 2006). One of the control structures that have advantages is that of droop control. The conventional droop control may be used to regulate the local voltage at the output of the inverter DG and allow operation of the shared active and reactive power flow required by the loads.

Droop control can be associated with other traditional structures. In Micallef *et al.* (2012) and Savaghebi *et al.* (2013), the droop is used to regulate the voltage and frequency, the PI controller can be used for active and reactive power cooperation between the inverters and the Proportional-Resonant controller can be used to compensate voltage harmonics in the coupling point.

In Kukandeh and Kazemi (2018) the individual droop control (P - f) and (Q - V) (two independent control loops) is evaluated in a microgrid connected and isolated from a low voltage network, where a PID regulator is also proposed to control the active powers and reactive provided by the inverter. In this scenario, closed-loop instability can compromise because the interaction between the loops is neglected.

The work in Anwar, Marei, and El-Sattar (2017) is proposing a hierarchical control structure for stable operation of an isolated microgrid, where the primary control is implemented full droop control voltage and frequency, and the secondary control is performed by the frequency control, which manages the reactive power-sharing in the inverters installed in MG.

2 Theoretical reference

Consider a simple MG, as shown in Figure 1. The distributed generator is a controlled power source for which one may dynamically adjust its amplitude (A) and frequency (f).

Figure 1 – Equivalent circuit of a DG unit connected to the common ac bus.

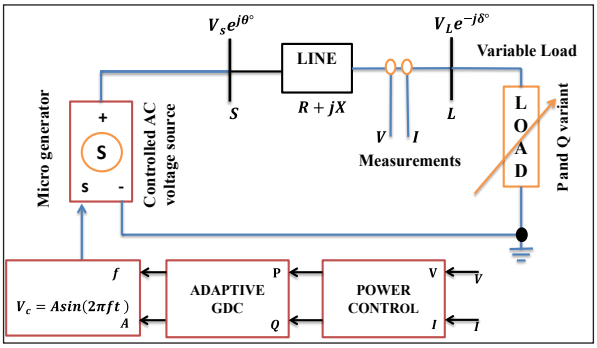

Source: Elaborated by the authors.

The distributed generator (DG) unit is connected to the L charge by the line impedance, Z. At the S point, the active (P) and reactive (Q) powers can be both expressed as follows (GUERRERO *et al*, 2007; BEVRANI; SHOKOOHI, 2013):

$$P = \frac{V_s^2}{Z}\cos\theta - \frac{V_s V_L}{Z}\cos(\theta - \delta) \quad (1)$$

and

$$Q = \frac{V_s^2}{Z}\sin\theta - \frac{V_s V_L}{Z}\sin(\theta - \delta) \quad (2)$$

where V_s and δ are the voltage generated and the phase angle of the voltage generated respectively, V_L is the voltage at the load and θ is the angle of the line impedance, Z. Considering $Z = ||Z||e^{j\theta} = R + jX$, the Equations (1) and (2) can be rewritten as,

$$P = \frac{V_s}{R^2 + X^2}[R(V_s - V_L\cos\delta) + XV_L\sin\delta] \quad (3)$$

$$Q = \frac{V_s}{R^2 + X^2}[-RV_L\sin\delta + X(V_s - V_L\cos\delta)] \quad (4)$$

The Equations (3) and (4) display the dependence of the voltage and the angle of the inverter output power with the active and reactive powers. Assuming a

mainly inductive electrical system ($Z \approx X$ and $\theta \approx 90º$), the fundamental active and reactive powers can be expressed as (BEVRANI; SHOKOOHI, 2013):

$$P \approx \frac{V_s V_L}{X} \sin \delta \quad (5)$$

$$Q \approx \frac{V_s V_L \cos \delta - V_L^2}{X} \quad (6)$$

In practical applications, δ is normally small; thus, a P/Q decoupling approximation ($cos\delta \approx 1$ and $sin\delta \approx \delta$) can be considered (GUERRERO *et al.*, 2007; HAGHSHENAS; EBADIN; SHARIATINASAB, 2014):

$$P \approx \frac{V_s V_L}{X} \delta \quad (7)$$

$$Q \approx \frac{(V_s - V_L) V_L}{X} \quad (8)$$

The vvEquations (7) and (8) show that in MGs with inductive behavior, the active power P must be controlled by the regulating δ and V_s is controlled by Q. Thus, the fundamental active and reactive powers can be controlled by the phase angle and magnitude of the DG unit output voltage, respectively. These strategies are known in the literature as, respectively, Q - V and P - f droop control techniques. These approximations are valid for shorter transmission lines (up to 80 km long) represented by an RL circuit, typical of low voltage distribution systems, which are inserted microgrid.

In this scenario the individual droop control Q - V and P - f can be characterized by (BEVRANI; SHOKOOHI, 2013):

$$f - f_0 = -k_p (P - P_0) \quad (9)$$

$$V_s - V_{s0} = -k_q (Q - Q_0) \quad (10)$$

where f_0 and V_{s0} are the nominal values of the MG voltage and frequency; P_0 and Q_0 are the control set-points for active and reactive power respectively; k_p and k_q are the droop controller coefficients for the DG active and reactive power.

For the general case for X and R (i.e., no approximated relationship) the instantaneous active and reactive powers ($P' = P_{measured}$ and $Q' = Q_{measured}$, instantaneous measurements) are represented (BEVRANI; SHOKOOHI, 2013):

$$P' = \frac{X}{Z} [K_f \Delta f + P_0 - K_R K_V \Delta V_s - K_R Q_0] \quad (11)$$

$$Q' = \frac{X}{Z} [K_R K_f \Delta f + K_R P_0 + K_V \Delta V_s + Q_0] \quad (12)$$

where $K_f = -1/k_p$, $K_R = R/X$, $K_V = -1/k_q$; Δ_f and ΔV_s are, respectively, the voltage and frequency deviations of the micro-generator. In Equations (11) and (12), the K_R index helps us to identify the voltage and frequency simultaneous control. After some algebraic manipulations from Equations (11) and (12) one may obtain

$$\Delta f = \frac{1}{K_f} \left(\frac{Z}{X} P' - P_0 \right) + \frac{K_R K_V}{K_f} \Delta V_s + \frac{K_R}{K_f} Q_0 \quad (13)$$

$$\Delta V_s = \frac{1}{K_V} \left(\frac{Z}{X} Q' - Q_0 \right) - \frac{K_R K_f}{K_V} \Delta f - \frac{K_R}{K_V} P_0 \quad (14)$$

From Equation (13) it is possible to observe that the K_f gain inversely alters (has effects on) the ΔV_s and Q_0 ponderation coefficients on the second and third terms, respectively.

Figure 2 (next page) illustrates the block diagram of the droop controller, described by Equations (13) and (14). Therefore, the controller has three gains, which must be tuned to adjust real-time fluctuations of voltage and frequency to legal conditions in response to the request for active and reactive power requested by the dynamic load.

One important feature of this controller is the fast accommodation of operational conditions on the occasion of an abrupt variation on the active and reactive power, setting the voltage and frequency fluctuations at the voltage source inverter (VSI) output.

Observing the block diagram of Figure 2 realizes the coupling between voltage and current control loops (green arrows), it is a cross-feedback system which determines the closed-loop stability. Thus, the choice of controller gains directly influences the stable operation of the MG in order to be obtained from the apparent power specification required by the load.

The output signals of the diagram of Figure 2 are the amplitude and frequency of the sinusoidal signal is compared with a triangular wave for generating the PWM (Pulse Width Modulation) used in the DC-AC converter thyristors. In other words, the Droop controller manages the energy delivered by the DG.

Figure 2 – Droop control block diagram.

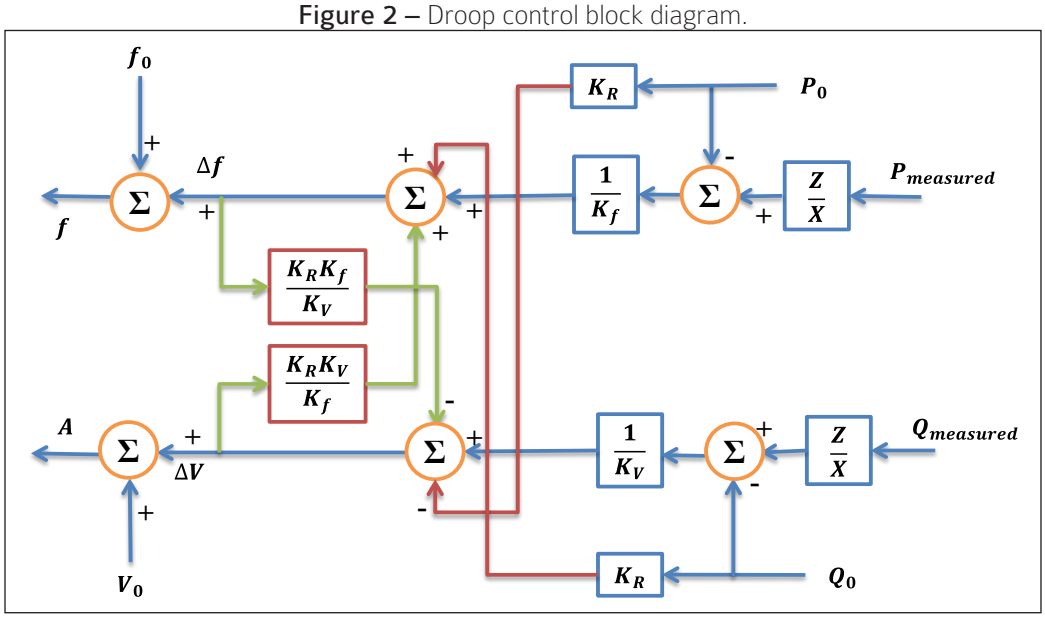

Source: Elaborated by the authors.

3 Research method

The methodology used for the design and tuning of the adaptive controller is discussed in this section and is divided into three subsections. The first subsection refers to the description of an adaptive droop control strategy that uses the structure of the self-tuning regulator. The second subsection details the online parameter estimator used to estimate the microgrid model seen from the DG terminals. The third subsection is dedicated to self-tuning the controller's gains (K_V, K_R, and K_f).

3.1 Description of the control strategy

The block diagram of the self-tuning adaptive control system is given in Figure 3.

Figure 3 – Block diagram of a self-tuning regulator.

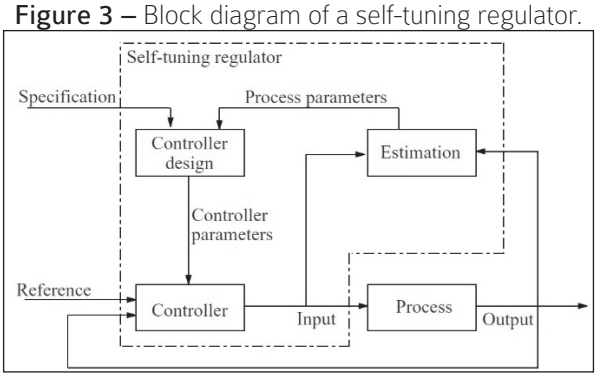

Source: Garrido and Moreno (2001).

In this case, the plant model is parameterized in terms of the controller parameter vector, the meeting closed-loop performance requirements. The recursive estimator calculates in real-time the parameters of the plant-based on the current state of the process from the input measurements (u) and output (y).

The estimated plant parameters are used for the controller re-design and are used to calculate new values for the control gains, so the controller is upgraded at the same pace of parameter estimator update calculation (self-tuning direct regulator).

The structure of self-tuning adaptive control has the necessary components for applying it in the stochastic setting. In the indirect structure, the parameters of the process are first estimated, and then the parameters of the regulator are designed, based upon the estimated process parameters.

The direct form unites these two steps in one, so the estimator gives automatically the parameters of the regulator, which must be given in the functional relation with process parameters. The advantage of the self-tuning structure is that it is capable of resolving many practical situations where there is no knowledge about the type of change the process would go through.

The block diagram of Figure 4 (next page) illustrates the adaptive Droop controller proposed. It is worth mentioning that this control structure installed at each DG unit; if there are n DG's present in the MG, there will be n local controllers.

Figure 4 – Block diagram for the proposed adaptive droop controller.

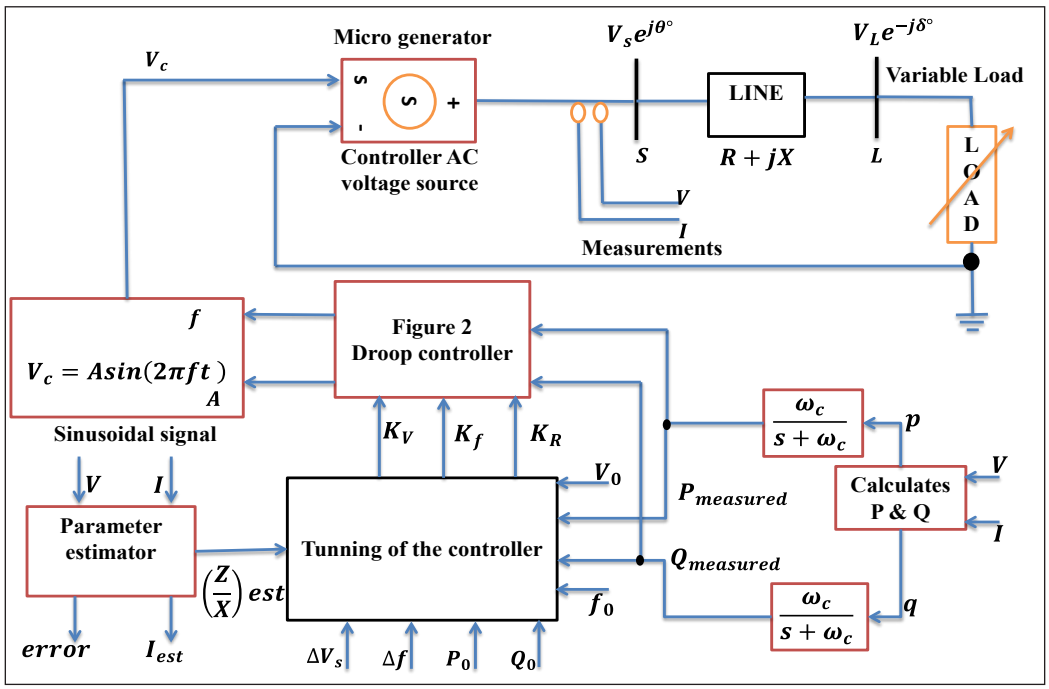

Source: Elaborated by the authors.

The controllers of each micro-generators interact with each other and with the central control located in the operation center through a low band bidirectional communications channel. This interaction was implemented through a state machine, allowing the active power-sharing among the several microgenerators installed in the MG.

Comparing the structure of the adaptive droop control (Figure 4) with the block diagram of the self-tuning regulator (Figure 3), it is noticed that it is the same structure. The process view is the microgrid of DG terminals (Thevenin equivalent); the block "parameter estimator" is the recursive estimator that calculates the Thevenin impedance from voltage and current measurements measured at the coupling point. The block called "tuning of the controller" is equivalent to the "design" block, where the controller gains are calculated, and then the values are sent to the block called the controller (structure of Figure 2).

The purpose of the control law is to provide the pure sinusoidal signal to be compared with the triangular signal to generate the PWM signal used on the keys (gate bus) of the DC-AC converter.

The control strategy works as follows:

(a) Measuring instruments are used to measure the instantaneous voltage and current values at the coupling point;

(b) With voltage and current values are calculated active and reactive power values supplied by DG to the microgrid, following these values are feedback to the controller (Figure 2) as well as the upgrade pack of control gains (controller parameters). The values of active and reactive powers are calculated as,

$$P_{measured} = VI\cos(\theta_V - \theta_I) \quad (15)$$

$$Q_{measured} = VI\sin(\theta_V - \theta_I) \quad (16)$$

where $P_{measured}$ and $Q_{measured}$ are the active and reactive powers measured instantly, V and I are, respectively, the voltage and current modules, and θ_V and θ_I are the angles of the voltage and current phases;

(c) The identification of the plant parameters is made in the block called "parameter estimator", this block receives the voltage and current measurements and returns the ratio (Z / X) to the controller design block, in addition to providing the error between the measured current and estimated current;

(d) The block called "tuning of the controller" is responsible for calculating instantly the K_f, K_V, and K_R gains from the current parameters of the plant ($a = Z$ / X), so this block receives the current data of the plant

and the values of powers injected into the microgrid and inform the droop controller the parameters (gains) of the controller;

(e) The block called "droop controller" is updated in real-time, following the dynamics of the loads present in the microgrid (input and output of consumers in the microgrid). In this way, the control is able to maintain the balance between generation and consumption. In the face of the controller, plant dynamics change the voltage or frequency values of the sine wave that is used to generate the PWM signal of the thyristors of the DC-AC converter pure sine wave.

All the blocks that compose the adaptive droop control structure are updated in the same sample rate, in the case in the microsecond order, which is a switching frequency of 10 kHz inverter keys in order.

3.2 Online parameter estimation

The recursive least squares estimator calculates the plant parameters in real-time, in other words, calculates the Thevenin impedance seen from the DG terminals (R and X) from the instantaneous measurements of voltage and current measured at the DG coupling point with the microgrid.

The parameter estimator takes into account the scenario described in Figure 5, the Thevenin equivalent seen from the load terminals for the circuit in Figure 1.

Figure 5 – Thevenin equivalent for frequencies of the h order.

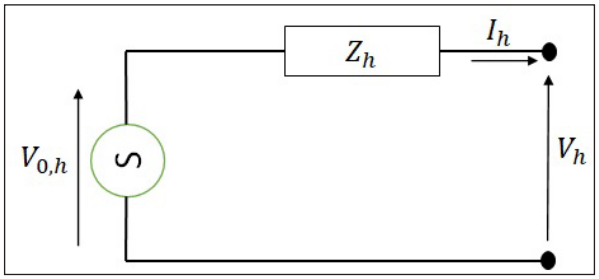

Source: Elaborated by the authors.

Considering an RLC circuit as the impedance seen from the DG terminals e applying the Kirchhoff's voltage law (for the fundamental frequency) to the circuit of Figure 5 we obtain,

$$V_{0,h}(s) = I_h(s)\left(R + sL + \frac{1}{sC}\right) + V_h(s) \quad (17)$$

as V_h is the open circuit voltage, then zero, where s denotes the Laplace operator. Rearranging the Equation (17) in terms of reactance (X),

$$V_{0,h}(s) = I_h(s)(R + sX) \quad (18)$$

To have a proper transfer function (the degree of denominator greater than the degree of the numerator), the output of the transfer function must be the electric current and the input voltage, given,

$$\frac{I_h(s)}{V_{0,h}(s)} = \frac{sC}{LCs^2 + sRC + 1} = Y_{est}(s) \quad (19)$$

The plant (microgrid view of the terminal DG) is given by a second-order model (Equation 19) where the RLC parameters are obtained from the parameter estimator. The RLS estimates the line impedance values and the parameter $a = Z / X$.

It is worth to notice that the estimated line impendence is given by $Z_{est}(s) = \frac{1}{Y_{est}(s)} = R_{est} + jX_{est}$, where X_{est} is the estimated inductive or capacitive reactance. Therefore, the estimator will provide two parameters, from the input voltage and current measured at the LCL filter output.

The system can be approximated by a second-order model, the difference equation, which represents the domain response of the discrete-time is given by Equation (20) where $u(k)$ and $y(k)$ are, respectively, input ($V_{0,h}$ measured) and output (I_h measured) signals; a_1, a_2 and b_0 are the parameters that define the dynamic behavior of the system.

$$y(k) = -a_1 y(k-1) - a_2 y(k-2) - b_0 u(k-1) \quad (20)$$

where line parameters are: $R_{est} = \frac{1}{a_1}$ and $X_{est} = \frac{1}{a_2}$.

The parameter $a = Z / X$ relative to the behavior of the microgrid, given the dynamic scenario of insertion or withdrawal of loads (consumers installed in the microgrid), is given by:

$$a = \frac{\|Z_{est}\|}{X_{est}} = \frac{\sqrt{(R_{est})^2 + (X_{est})^2}}{X_{est}} \quad (21)$$

The RLS algorithm does not need a database to finally estimate the parameters. The parameters are recursively estimated for each newly available output and input value, for this purpose, the measurement matrices φ and output Y are constantly updated.

Using Equation (22) the parameters are calculated and updated, where ε is the prediction error and H is the estimator gain matrix (RAMOS, 2015). The Equations (23) to (29) assist in the estimation process (LJUNG, 1999; AGUIRRE, 2004).

$$\varphi(k) = M^t \tag{22}$$

$$M = [-y(k-1)\ldots -y(k-n)\ u(k-1)..u(k-n)] \tag{23}$$

$$Y = [y(0)\quad y(1)\quad y(2)\quad \ldots\quad y(n-1)]^t \tag{24}$$

$$\theta = [a_1\quad \ldots\quad a_2\quad b_1\quad \ldots\quad b_n]^t \tag{25}$$

$$\theta(k) = \theta + H\varepsilon(k) \tag{26}$$

$$\varepsilon(k) = Y - \varphi^t\theta \tag{27}$$

$$H(k) = \frac{P\varphi}{1+\varphi^t P\varphi} \tag{28}$$

$$P(k) = P - H\varphi^t\varphi \tag{29}$$

where $P(k)$ is the covariance matrix, which must be initialized with a unit value and θ is the estimated parameter vector.

3.3 Controller design

The adjustment of the gains of the adaptive droop controller is motivated by the DG operating conditions and the MG restrictions for the voltage and frequency levels imposed by the Brazilian standard NBR 5410/2004. The block of Figure 6 was designed to determine the optimal gains of the droop controller in Figure 2.

Figure 6 – Adaptive tuning of the block.

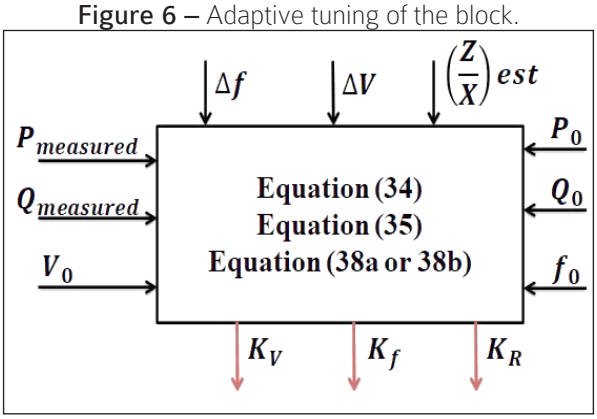

Source: Elaborated by the authors.

The block in Figure 6 receives as input, the reactive and active powers measured in the electrical network; the tolerable minimum and maximum values for the operating voltage and frequency ($\Delta_f = \pm 1$ Hz and $\Delta V_s = \pm 10$ V; the control set-points of the active power (P_0), of the reactive power (Q_0), frequency (f_0), voltage (V_0); and the estimated line parameters. As to the output, the block provides the K_v, K_R, K_f and controller gains.

The operating conditions determine the operational regions (2D regions) of the PQ and Af distributed generation, as shown in Figure 7.

Figure 7 – and operational regions.

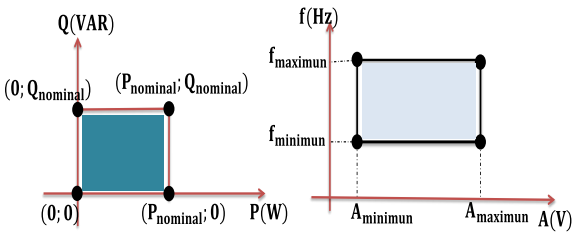

Source: Elaborated by the authors.

From the individual droop control P-f and Q-V droop definition,

$$K_f = -\frac{1}{k_p} \therefore k_p = -\frac{1}{K_f} \tag{30}$$

$$K_V = -\frac{1}{k_q} \therefore k_q = -\frac{1}{K_V} \tag{31}$$

Substituting the Equations (30) and (31) into Equations (9) and (10),

$$\Delta f = -k_p(P' - P_0) \rightarrow \Delta f = \frac{1}{K_f}(P' - P_0) \tag{32}$$

$$\Delta V_s = -k_q(Q' - Q_0) \rightarrow \Delta V_s = \frac{1}{K_V}(Q' - Q_0) \quad (33)$$

Isolating K_V and K_f, it follows as,

$$K_f = \frac{(P' - P_0)}{\Delta f} \quad (34)$$

$$K_V = \frac{(Q' - Q_0)}{\Delta V_s} \quad (35)$$

where $P' = P_{measured}$ and $Q' = Q_{measured}$ are the active and reactive powers measured instantly.

According to the concept of droop control, the K_R gain is a variable influenced by the line parameters, especially by the dissipative effect of the line (Joule effect). Applying the Equations (32) and (33) in the Equations (13) and (14) respectively, it follows as,

$$\Delta f - \frac{1}{K_f}(aP' - P_0) = K_R Q_0 \quad (36a)$$

$$\Delta V_s - \frac{1}{K_V}(aQ' - Q_0) = -K_R P_0 \quad (36b)$$

Substituting K_v and K_f into (36a) and (36b),

$$K_R Q_0 = \Delta f - \frac{\Delta f(aP' - P_0)}{(P' - P_0)} \quad (37a)$$

$$K_R P_0 = \frac{\Delta V_s(aQ' - Q_0)}{(Q' - Q_0)} - \Delta V_s \quad (37b)$$

Isolating $K_{R'}$

$$K_R = \frac{\Delta f}{Q_0}\left[1 - \frac{(aP' - P_0)}{(P' - P_0)}\right] = K'_R \quad (38a)$$

$$K_R = \frac{\Delta V_s}{P_0}\left[\frac{\Delta V_s(aQ' - Q_0)}{(Q' - Q_0)} - 1\right] = K''_R \quad (38b)$$

where $a = Z / X$, the parameter used to evaluate the behavior of MG (inductive or capacitive).

Equation (38) shows that the K_R gain can be adjusted by the active power, as well as by the reactive power, or that it can be calculated as an arithmetic mean of the two values.

To set the 3D control region for the K_V, $K_{R'}$ and K_f gains, it is necessary to evaluate the extremes of the operational region, setting the minimum and maximum values.

Evaluating minimum and maximum K_f values,

$$P_0 = 0W \rightarrow K_{f_{max}} = \frac{P'}{\Delta f} \quad (39a)$$

$$P_0 = P_{nominal} \rightarrow K_{f_{min}} = \frac{P' - P_{nominal}}{\Delta f} \quad (39b)$$

Evaluating minimum and maximum K_V values

$$Q_0 = 0\,VAR \rightarrow K_{V_{max}} = \frac{Q'}{\Delta V_s} \quad (40a)$$

$$Q_0 = Q_{nominal} \rightarrow K_{V_{min}} = \frac{Q' - Q_{nominal}}{\Delta V_s} \quad (40b)$$

Evaluating minimum and maximum K_R values from the active power,

$$P_0 = 0W \rightarrow K_{R_{max}} = \frac{\Delta f}{Q_0}(1 - a) \quad (41a)$$

when the active power set-point is equal to the nominal power value, the gain K_R is:

$$K_{R_{min}} = \frac{\Delta f}{Q_0}\left(1 - \frac{aP' - P_{nominal}}{P' - P_{nominal}}\right) \quad (41b)$$

Evaluating K_R minimum and maximum values from the reactive power,

$$Q_0 = 0\,VAR \rightarrow K_{R_{max}} = \frac{\Delta V_s}{P_0}(a - 1) \quad (42a)$$

when the reactive power set-point is equal to the value of the nominal reactive power, the gain K_R is:

$$K_{R_{min}} = \frac{\Delta V_s}{P_0}\left(\frac{aQ' - Q_{nominal}}{Q' - Q_{nominal}} - 1\right) \quad (42b)$$

The quality of the controller setting is associated with the quality of the estimate of the line parameters.

This is the case because K_f and K_V gains are influenced, respectively, by the active and reactive power. While the gain K_R is dependent on the active power or reactive power, it is also influenced by the line parameters.

4 Results and discussion

This section presents the results of the simulation droop control strategy proposed when evaluated in three microgrids configuration, focusing on

the dynamics of the closed-loop system for the management of energy flow.

4.1 1-bus test MG

Firstly, the adaptive droop control was evaluated with a simple MG (Figure 1), the purpose of the control strategy is simultaneously regulating the MG's voltage and frequency during the supply of the apparent power for the DG local charge, assuring the generation-consumption balance in a quick, safe and stable manner.

Table 1 maps the active and reactive power profile representing the local variable load into resistance and reactance values (inductive or capacitive).

Table 1 – Load mapping in R and X values.

Time instant (s)	($S = P + jQ$) [kVA]	Impedance (Ω)
0.0 – 2.0s	$2 + j1$	$0.1 + j1$
0.2 – 1.6s	$2 - j1$	$0.1 - j1$
0.4 – 1.4s	$2 + j1$	$0.1 + j0.5$
0.6 – 1.2s	$2 + j1$	$0.1 + j1$
0.8 – 1.0s	$2 + j1$	$0.1 + j1$

Source: Authors data.

The apparent power values in Table 1 were defined based on the 8 kVA/220V sinusoidal photovoltaic inverters available on the market.

Observing the control response (Figure 8) generated to regulate the voltage and frequency of the microgrid, one may notice that the microgrid is operating within the region allowed by the legislation, NBR 5410 and IEEE 1547, (voltage - upper limit of 341 V_{PP} and lower limit of 281 V_{PP}; frequency - upper limit of 61 Hz and lower limit of 59 Hz), since the minimum value verified for the voltage in the bar was $V_{PP} = 295\ V$.

The objective of the control action is to maintain the operation of the MG within this operating range.

In Figure 9 illustrates the balance between generation and consumption when managed by the adaptive droop, it can be seen that the inverter effectively meets the energy demand of the local load, both in the load insertion intervals, as well as in the withdrawal time periods local charge.

Figure 10 shows that the least-squares estimator was able to estimate the output current of the inverter, but during the first half of the simulation (1 second) the error varied by 20 units, already in the second half the error was practically null.

It is noticed that when there is a sudden switching of a load with an apparent power value much higher than the previous apparent power value (for example, $S_{before} = 3 + j1$ kVA and changes to $S_{after} = 6 + j3$ kVA), the RLS cannot follow the estimation in real-time, presenting a larger error.

Figure 8 – 1-bus voltage and frequency profiles.

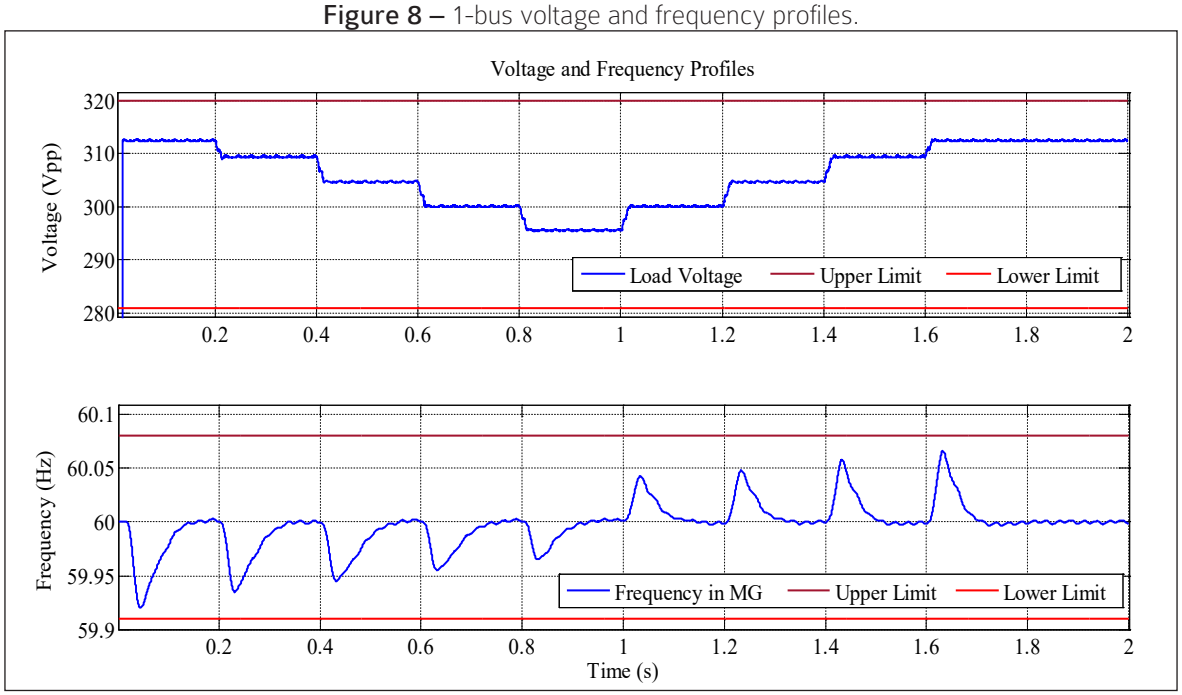

Source: Authors data.

Figure 9 – Generation and consumption profile.

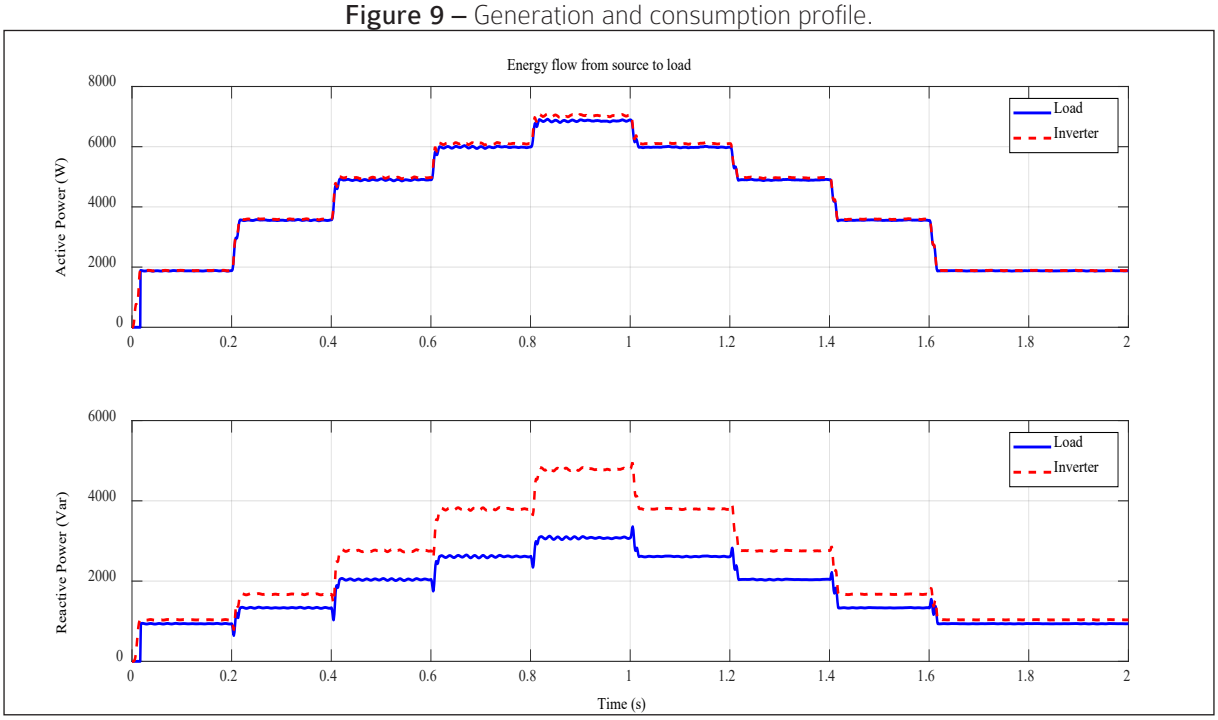

Source: Authors data.

Figure 10 – Estimated current versus estimated current and the estimation error.

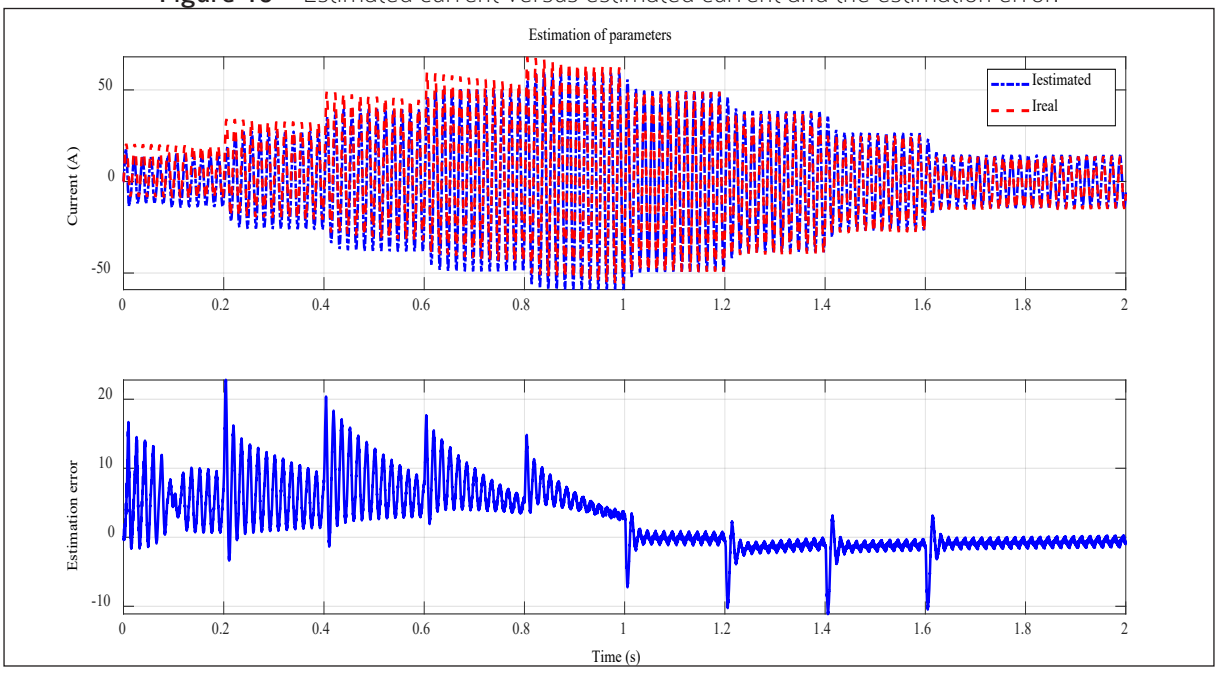

Source: Authors data.

This fact can be explained by Equation (20) since the derivative of the step function results in the impulse function because the MG does not tolerate rapid changes in current ($dI\ /\ dt$) or voltage ($dV\ /\ dt$), but even in this scenario, the estimator and the optimum tuning work well, keeping MG stable.

The current profile, it is observed that its behavior is analogous to the dynamic load profile, from 0.2 seconds to 1 second the current increases, as well as the active power profile. According to 2.0 seconds, the current decreases returning to the initial conditions (before 0.2 seconds).

Figure 11 shows the behavior of the parameter Z / X provided by RLS and used in controller design. The value of a is unitary or close to one because the value of the reactance (imaginary part of the impedance) is much higher than the value of the real part of the impedance (resistance). Therefore, Z is next to X, and $a = Z / X \approx 1$.

Figure 11 – Impedance module divided by reactance.

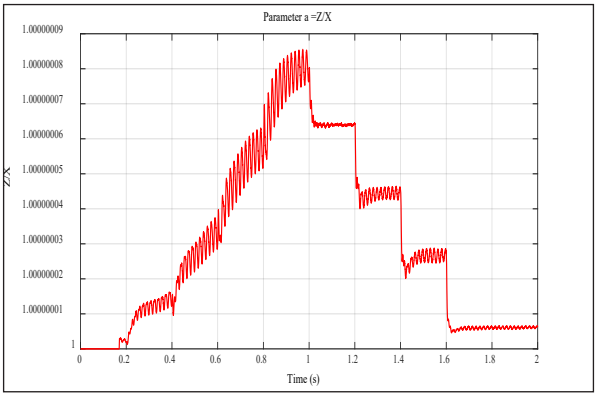

Source: Authors data.

Figure 12 shows the estimated impedance (R and X) values for the 1-bus MG case study, with the parameter X (reactance) illustrates the behavior of the microgrid in relation to the consumer profile (inductive or capacitive).

Figure 12 – Estimated R and X parameters.

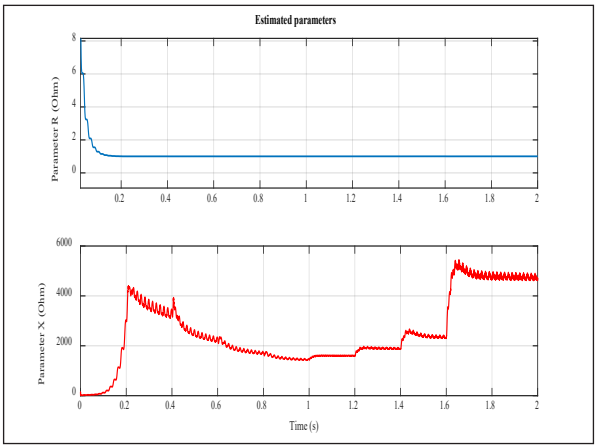

Source: Authors data.

4.2 3-bus test MG

In order to test and evaluate the effectiveness of the adaptive droop control, it was initially evaluated in the three-bus MG shown in Figure 13 with loads with a purely inductive behavior considering: 0.6 kW initially for load 1, located in bus 1 and 0.2 kW initially for load 2, located in bus 3.

Figure 13 – MG with three DG's and two load banks.

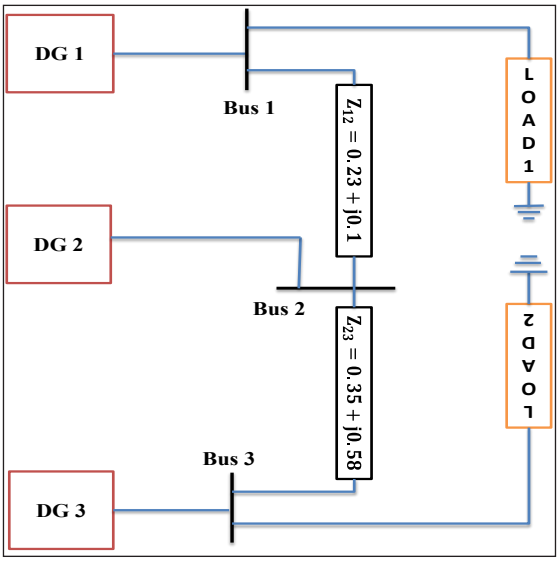

Source: Elaborated by the authors.

It should be noted that the nominal apparent power at the inverter output (control references) of each micro-generator considered was of the $S = 3 + j0.85$ kVA, because during load-bank switching, consumer demand $S = 1 + j0.8$ kVA.

The problem in question is to assess the capacity of the controller proposed to maintain the power balance between generation and efficient, reliable consumption and meeting consumer demand, in view of the load change scenario as well as to evaluate the performance of MG operating in islanding mode.

Figure 14 illustrates the behavior (profiles) of voltage and frequency when the adaptive droop control evaluated in the 3-bus MG.

Observing the Figure 14 (next page) the MG operates within the prescribed values for voltage and frequency fluctuations, operating between $\Delta V_{DG1} = \pm 10$ V, $\Delta V_{DG2} = \pm 6$ V and $\Delta V_{DG3} = \pm 5$ V for tensions and between $59.85 \text{ Hz} \leq f \leq 60.15$ Hz, $\Delta f = \pm 0.3$ Hz for frequency deviations. Faced with the dynamic scenario the controller managed to fulfill the established objectives: to manage the MG operation stable and faithfully meeting the consumer's profile.

Figure 14 – 3-bus voltage and frequency profiles.

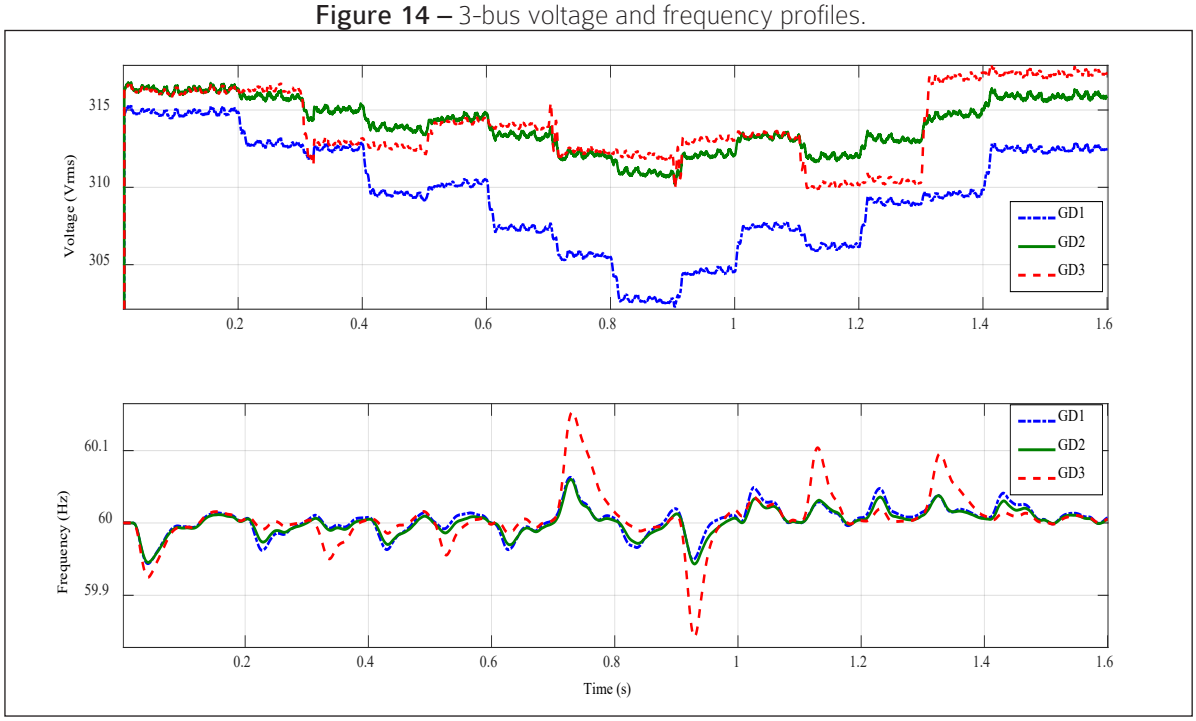

Source: Authors data.

4.3 14-bus test MG

In order to test and evaluate the effectiveness of the adaptive droop control, it was evaluated in the IEEE 14-bus MG (Figure 15).

Figure 15 – 14-bus microgrid.

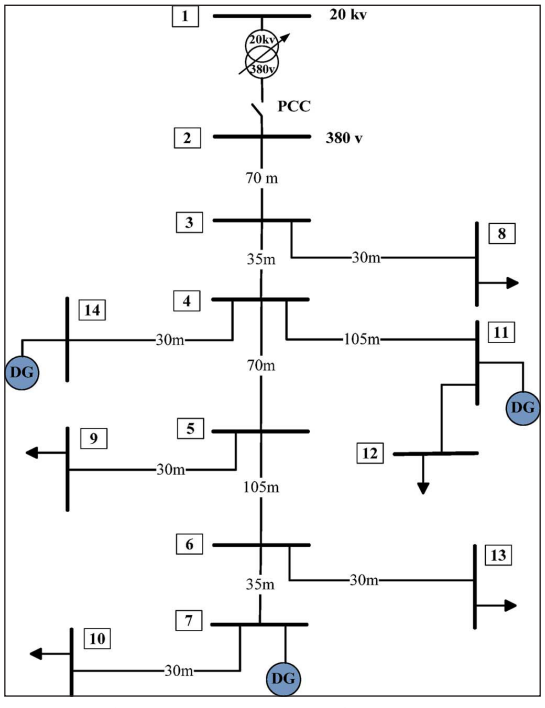

Source: Papathanassiou, Hatziargyriou and Strunz (2005).

The dynamic loads connected to buses 7, 8, and 9, and their respective switching times are shown in Table 2. The fixed load values connected to these buses shown in Table 3.

The loads in Tables 2 and 3 were fixed by the authors in the simulations, assuming apparent power values within the operational limits of the low voltage network brought in by Papathanassiou Hatziargyriou and Strunz (2005).

Table 2 – Variables loads connected in the 14-bus MG.

Time instant (*s*)	Load 1 in bus 8 [kVA]	Load 2 in bus 9 [kVA]	Load 3 in bus 7 [kVA]
0 – 0.3	3	2	3
0.3 – 0.5	5 + *j*2	4 + *j*2	3 + *j*1.5
0.5 – 0.7	8 + *j*3	6	2.5
0.7 – 0.9	6	*j*2	*j*1.5
0.9 – 1.1	4 + *j*2.5	5	4
1.1 – 1.3	2 + *j*2	4 + *j*2	5 + *j*3

Source: Authors data.

The voltage and frequency profiles for this scenario illustrated in Figure 16 (next page). The microgrid operates within the operational range prescribed by law, showing fluctuations of ±10 V for voltage and ±0.02 Hz for frequency.

Figure 16 – 14-bus voltage and frequency profiles.

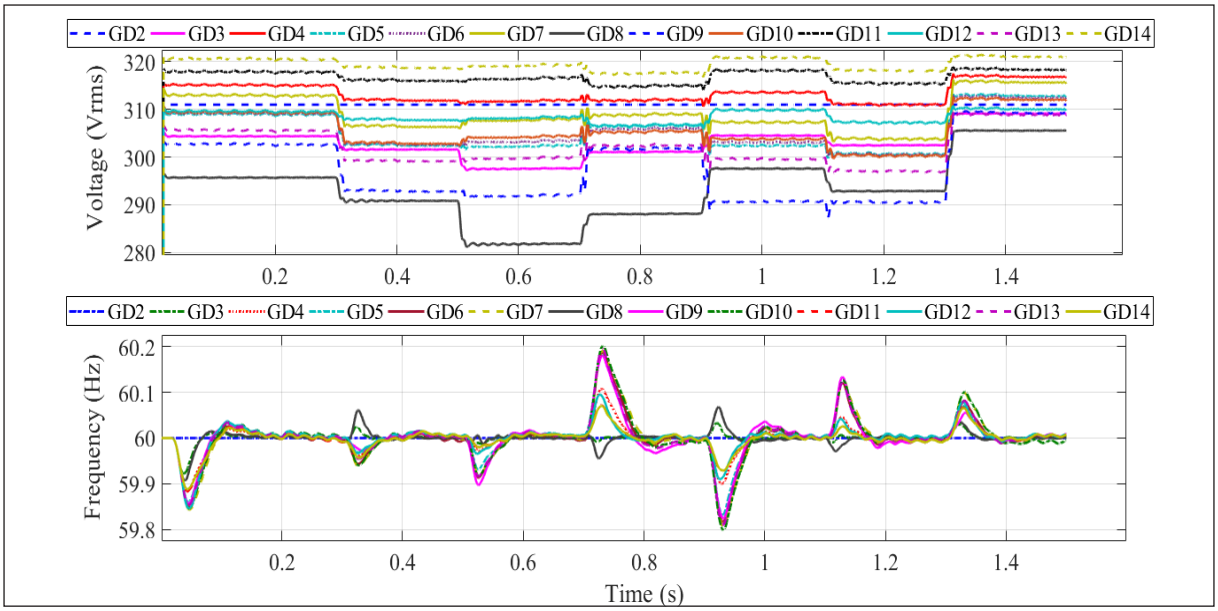

Source: Authors data.

Table 3 – Fixed loads connected in the 14-bus MG.

Bus	Load (kVA)
8	$2 + j1$
9	$2.5 + j0.5$
10	$5 + j2.5$
12	$2 + j1$

Source: Authors data.

The adaptive droop controller showed a quick response to the operational changes imposed by the dynamic load scenario, MG operation in a stable and safe closed-loop, maintaining the balance between the generation and consumption.

4.4 Discussion of the proposed control strategy

The closed-loop dynamics are dictated by the gains of the droop controller (K_V, K_f, and K_R) determined by the adaptive law from the apparent power demanded by the consumer.

The K_V gain is responsible for the dynamics of the control system, ensuring error null steady state, a large amount of K_V leads to a slow response of the controller against the apparent power demand required by the load since a small amount of K_V leads to quick system response, but with the introduction of overshoot.

The K_R gain eliminates the oscillations of the control response against the apparent power of reference as well as reduces or increases the overshoot, the greater the K_R value, the greater will be the overshoot, otherwise, there will be a reduction in overshoot.

Finally, the K_f gain, this takes the control response to proximity to the apparent power demand requested by the load, accelerating the controller response (10 times the MG dynamics).

The cross-feedback (the products $\Delta f K_R K_f$ and $\Delta V_s K_R K_V$) from the controller outputs to the control structure will define the controller establishment time, in other words, the speed of the control.

An analogy can be made between the PID controller with the droop control, being K_V gain equivalent to the integral action, the K_f gain equivalent to proportional action, and derivative action equivalent to K_R.

The proposed controller offers the following advantages for the operation of the MG:

(a) It reduces the dependency of isolated microgrids on energy storage systems to regulate the active power mismatch, and hence frequency;

(b) It facilitates nominal steady-state frequency operation;

(c) Without the need for additional controls;

(d) It works with any type of DG, i.e., converter and machine-based, with voltage control capability, maintaining voltages within acceptable ranges;

(e) Only local feedback signals are required, i.e., there is no need for communications;

(f) It improves the system damping.

The controller structure designed so that the DG's work cooperatively to meet the energy demand of local loads. A negative point is the fact that the parameter estimator performs many calculations, demanding more efficient hardware and software structure.

5 Conclusions

In this paper proposed and validated one adaptive control strategy for simultaneous regulation of voltage and frequency at the inverter output in microgrids. The strategy uses the structure of the traditional droop controller (Q - V and P - f), associated with the parametric identification in the real-time estimation line impedance and the optimum tuning of the controller's gains.

The adaptive droop controller solves the problem of dependence on conventional droop with the parameters of the power line, obtaining optimum performance in closed-loop and quick response to load disturbances.

The controller is simple, has a straightforward implementation, and is easily applicable to a variety of different systems and voltage regulation devices.

The adaptive droop can be very effective in minimizing the impact of large disturbances on the system such as loss of a generation, enhancing small-perturbation stability by providing more damping for the system.

The controller also requires no additional investment or communication infrastructure. By presenting rapid response, so the voltage and frequency provided by DG maintained within acceptable operating limits, avoiding a negative impact on the quality of service for the customer. However, its performance depends on the characteristics of the consumers and the supply voltage ranges.

The strategy was able to stabilize the voltage and the frequency of inverters output when evaluated in several topologies of MG and different scenarios of load tests in closed-loop, maintaining the balance between generation-consumption and meeting the legal operational requirements.

REFERENCES

AGUIRRE, L. A. **Introdução à identificação de sistemas**: técnicas lineares e não-lineares aplicadas a sistemas reais. 2. ed. Belo Horizonte (Brasil): Ed. UFMG, 2004. In Portuguese.

ANWAR, M.; MAREI, M. I.; EL-SATTAR, A. A. Generalized droop-based control for an islanded microgrid. In: 2017 12th INTERNATIONAL CONFERENCE ON COMPUTER ENGINEERING AND SYSTEMS (ICCES), 2017, Cairo (Egypt). **Proceedings**... 2017.

ASSOCIAÇÃO BRASILEIRA DE NORMAS TÉCNICAS. ABNT NBR 5410: 2004 versão corrigida 2008. Rio de Janeiro (Brasil): ABNT, 2004. In Portuguese.

BALAGUER, I. J. *et al.* Control for grid-connected and intentional islanding operations of distributed power generation**. IEEE Transactions on Industrial Electronics**, v. 58, n. 1, p. 147-157, 2011.

BEVRANI, H.; SHOKOOHI, S. An intelligent droop control for simultaneous voltage and frequency regulation in islanded microgrids, **IEEE Transactions on Smart Grid**, v. 4, n. 3, p. 1505-1513, 2013.

FU, Q. *et al.* Microgrid generation capacity design with renewables and energy storage addressing power quality and surety. **IEEE Transactions on Smart Grid**, v. 3, n. 4, p. 2019-2027, 2012.

GARRIDO, S.; MORENO, L. Learning adaptive parameters with restricted genetic optimization method. In: MIRA J.; PRIETO, A. (eds) **Connectionist Models of Neurons, Learning Processes, and Artificial Intelligence. IWANN 2001. Lecture Notes in Computer Science**, v. 2084. Berlin (Germany): Springer, 2001.

GUERRERO, J. M. *et al.* Decentralized control for parallel operation of distributed generation inverters using resistive output impedance. **IEEE Transactions on Industrial Electronics**, v. 54, n. 2, p. 994-1004, 2007.

GUERRERO J. M. *et al.* Hierarchical control of droop-controlled AC and DC micro grids: a general approach toward standardization. **IEEE Transactions on Industrial Electronics**, v. 58, n. 1, p. 158-172, 2011.

HAGHSHENAS, M.; EBADIN, M.; SHARIATINASAB, R. Autonomous control of inverter-interfaced distributed generation units for power quality enhancement in islanded microgrids. **International Journal of**

Mechatronics, Electrical and Computer Technology (IJMEC), v. 4, n. 10, p. 1247-1271, 2014.

INSTITUTE OF ELECTRIC AND ELECTRONICS ENGINEERS. IEEE 519-2014: Recommend Practice and Requirements for Harmonics Control in Electric Power Systems, IEEE, 2014.

INSTITUTE OF ELECTRIC AND ELECTRONICS ENGINEERS. IEEE. IEEE 1547-2003: IEEE standard for interconnecting distributed resources with electric power systems, IEEE, 2003.

KUKANDEH, Y. R.; KAZEMI, M. H. Microgrid control in islanding and connected mode. In: IRANIAN CONFERENCE ON ELECTRICAL ENGINEERING (ICEE), 2018, Mashhad (Iran). **Proceedings...** 2018.

LJUNG L. **System identification**: theory for the use. 2 Ed. New Jersey (United States): Prentice-Hall, 1999.

LOPES, J. A. P; MADUREIRA, C. L.; MADUREIRA, A. G. Defining control strategies for microgrids islanded operation. **IEEE Transactions on Power Systems**, v. 21, n. 2, p. 916–924, 2006.

MAJUMDER, R. *et al*. Load sharing and power quality enhanced operation of a distributed microgrid. **IET Renewable Power Generation**, v. 3, n. 2, p. 109-119, 2009.

MARWALI, M. N.; KEYHANI, A. Control of distributed generation systems – Part I: voltages and currents control. **IEEE Transactions on Power Electronics**, v. 19, n. 6, p. 1541-1550, 2004.

MICALLEF, A. *et al*. Secondary control for reactive power sharing in droop-controlled islanded microgrids. In; 2012 IEEE INTERNATIONAL SYMPOSIUM ON INDUSTRIAL. ELECTRONICS, 2012, Hangzhou (China). **Proceedings...** 2012. p. 1627–1633.

MOHAMED, Y. A. R. I.; EL-SAADANY, E. F. Adaptive decentralized droop controller to preserve power sharing stability of paralleled inverters in distributed generation micro grids. **IEEE Transactions Power Electronics**, v. 23, n. 6, p. 2806-2816, 2008.

PAPATHANASSIOU, S.; HATZIARGYRIOU, N.; STRUNZ, K. A benchmark low voltage microgrid network. In: CIGRE SYMPOSIUM "POWER SYSTEMS WITH DISPERSED GENERATION; TECHNOLOGIES, IMPACTS ON DEVELOPMENT, OPERATION AND PERFORMANCES, 2005, Athens (Greece). **Proceedings**... 2005.

RAMOS, A. C. **Identificação de sistemas dinâmicos aplicada:** desenvolvimento de software baseado em mínimos quadrados. 2015. 75 f. Dissertação (Mestrado Profissional). Instituto de Tecnologia, Universidade Federal do Pará, Belém (Brasil), 2015. In Portuguese.

SAVAGHEBI, M. *et al*. Autonomous voltage unbalance compensation in an islanded droop-controlled microgrid. **IEEE Transactions on Industrial Electronics**, v. 60, n. 4, p. 1390-1402, 2013.

ZHENGBO, M.; LINCHUAN, L.; TUO, D. (2011). Application of a combined system to enhance power quality in an island microgrid. In: 2011 IEEE POWER ENGINEERING AND AUTOMATION CONFERENCE, Wuhan (China), 2011. **Proceedings...** 2011. p. 326-330.

ZHONG, Q.-C. Robust droop controller for accurate proportional load sharing among inverters operated in parallel. **IEEE Transactions Industrial Electronics**, v. 60, n. 4, p. 1281-1290, 2011.